

Theoretical Investigation of CO Interaction with Copper Sites in Zeolites: Periodic DFT and Hybrid Quantum Mechanical/Interatomic Potential Function Study

Ota Bludský, Martin Silhan, and Petr Nachtigall*

Center for Biomolecules and Complex Molecular Systems, Institute of Organic Chemistry and Biochemistry, Academy of Sciences of the Czech Republic, Flemingovo n. 2, CZ-16610 Prague, Czech Republic

T. Bucko, L. Benco,[†] and J. Hafner*

Institut für Materialphysik and Center for Computational Material Science, Universität Wien, Sensengasse 8, A-1090 Wien, Austria

Received: February 6, 2005; In Final Form: March 11, 2005

Periodic DFT and combined quantum mechanics/interatomic potential function (QM-pot) models were used to describe the interaction of CO with the Cu⁺ sites in FER. The CO stretching frequencies were calculated using $\omega_{\text{CO}}(\text{CCSD(T)})/r_{\text{CO}}(\text{DFT})$ scaling method relating frequencies determined using a high-level quantum-chemical (coupled clusters) method for simple model carbonyls to CO bond lengths calculated using periodic DFT and QM-pot methods for the Cu⁺–zeolite system. Both periodic DFT and QM-pot models together with $\omega_{\text{CO}}/r_{\text{CO}}$ scaling describe the CO stretching dynamics with the “near spectroscopic accuracy”, giving $\nu_{\text{CO}} = 2156 \text{ cm}^{-1}$ in excellent agreement with experimental data. Calculations for various Cu⁺ sites in FER show that both types of Cu⁺ sites in FER (channel-wall sites and intersection sites) have the same CO stretching frequencies. Thus, the CO stretching frequencies are not site-specific in the CO/Cu⁺/FER system. The convergence of the results with respect to the model size was analyzed. When the same exchange-correlation functional is used the adsorption energies from periodic DFT and QM-pot are in good agreement (about 2 kcal/mol difference) but substantially larger than those of the experiment. The adsorption energy calculated with the B3LYP functional agrees with available experimental data. The overestimation of the adsorption energy in DFT calculations (periodic or QM-pot) is related to a red-shift of the CO stretching mode, both result from an underestimation of the HOMO(5 σ)-LUMO(2 π^*) gap of CO and the consequent overestimation of the Cu⁺(d)-CO(2 π^*) back-donation. For the adsorption energy, this can be overcome by the use of hybrid B3LYP exchange-correlation functional. For the frequency calculations, the DFT problem can be overcome by the use of the $\omega_{\text{CO}}(\text{CCSD(T)})/r_{\text{CO}}(\text{DFT})$ correlation.

1. Introduction

Information about the structure and coordination of extraframework metal cations in high-silica zeolites is very difficult to obtain from X-ray diffraction experiments. Instead, IR spectra of probe molecules adsorbed on the metal cation (M⁺) are often used for characterization of M⁺/zeolite systems. Carbon monoxide is a particularly suitable probe molecule due to a high sensitivity of the vibrational dynamics of adsorbed CO to the coordination environment of the metal cation.¹ Cu⁺ exchanged zeolites are among the most intensively studied M⁺/zeolite systems since Iwamoto's discovery of unusually high activity of Cu⁺/ZSM-5 in the deNO_x process.²

The IR spectra of CO/Cu⁺/zeolite systems show CO stretching frequencies in the range 2122–2160 cm^{−1} depending on the zeolite structure.^{3–5} These frequencies are either red- or blue-shifted with respect to gaseous CO (2143.5 cm^{−1}). It was suggested that the red-shift is due to the increased electron density on Cu⁺ caused by H₂O or NH₃ co-ligands.^{6,7} The blue-shift of the CO stretching frequencies upon the CO adsorption on Cu⁺/zeolites was explained by various phenomena: (i)

σ -donation dominates π -back-donation in nonclassical copper carbonyls,^{8,9} (ii) the effect of the Madelung potential,¹⁰ and (iii) the repulsive interaction of CO with the framework atoms on the opposite side of the channel.¹¹

The changes in the stretching frequencies of CO adsorbed on Cu⁺/zeolites were investigated theoretically using normal-mode analysis for small cluster models at the density functional theory (DFT) level.^{12,13} These models fail to reproduce the experimentally observed blue-shift of the CO frequency upon adsorption on Cu⁺/zeolite. Even more sophisticated embedding models employed recently do not give an unambiguous explanation of the CO frequency blue-shift. Treesukol et al. used the electrostatic embedding model for the description of the CO/Cu⁺/ZSM-5 system and concluded that the blue-shift of the CO frequency is due to a Madelung effect.¹⁰ This conclusion was questioned by Davidova et al., who used a mechanical embedding model and concluded that the CO frequency blue-shift cannot be correctly reproduced at the DFT level.¹⁴ The DFT frequencies show a systematic error, and therefore, empirical scaling factors are often used to obtain a better agreement with experimental data.¹⁵ However, a uniform empirical scaling can hardly account for a wrong sign of the CO frequency shift upon adsorption. The difficulty in describing the frequency spectrum of CO adsorbed in Cu⁺–zeolites (and in zeolites containing

* To whom correspondence should be addressed. Tel: +420-220-410-314. Fax: +420-220-410-320. E-mail: petr.nachtigall@uochb.cas.cz.

[†] On the leave from the Institute of Inorganic Chemistry, Slovak Academy of Sciences, Bratislava, Slovak Republic.

transition-metal cations) using DFT techniques is striking since there is ample evidence that DFT calculations correctly reproduce the stretching frequency blue-shift of the CO adsorbed on various cations, including Brönsted OH groups,^{16,17} surface silanol groups, extraframework Al³⁺ ions, alkali cations,¹⁶ polyvalent simple metal ions (Zn²⁺), and even heavier noble metal cations such as Ag⁺.¹⁸

The potential sources of errors in the description of the CO stretching dynamics in CO–Cu⁺/zeolite systems were recently analyzed by some of us.¹¹ The following aspects of the model were considered: (i) the proper description of the CO vibrational dynamics including anharmonic effects, (ii) the reliability of the quantum chemical methods employed in the electronic structure calculations, and (iii) the size and topology of the zeolite model. The use of the harmonic approximation for the description of the CO stretching vibration does not represent a major problem since the anharmonic corrections are nearly the same for the gas-phase CO and for the Cu⁺CO species (–29 cm^{–1}).¹⁹ The CO frequencies cannot be accurately described at the DFT level of theory for CO–Cu⁺X species. The use of GGA-type exchange-correlation functionals is problematic for the calculation of the CO···Cu⁺ interaction energies since these functionals overestimate bonding (e.g., PBE functional gives –46 kcal/mol for the gas-phase Cu⁺CO, including BSSE and ZPE corrections). On the contrary a hybrid B3LYP functional gives interaction energy in excellent agreement with experiment (–35.4 and –35.5 kcal/mol, respectively).^{20,21} Since GGA functionals overestimate the Cu⁺–CO bond (about 10 kcal/mol), they cannot be used for the calculation of CO adsorption energies in Cu⁺/zeolites. The overestimation of adsorption energies and the red shift of the CO frequencies at the DFT level is a manifestation of the general tendency of the DFT approach to overbind. This tendency is even much stronger at the LDA level, but it persists also at the GGA level. For CO adsorbed on metal cations, there is a particular aspect, which adds to this difficulty, namely the underestimation of the HOMO–LUMO gap. The interaction of CO with the substrate is determined by a delicate equilibrium between donation from the occupied 5σ (HOMO) state to the substrate and back-donation to the empty 2π* (LUMO) state. The underestimation of the HOMO–LUMO gap favors back-donation to the antibonding 2π* level and hence a stronger adsorbate–substrate interaction, as well as a weaker CO bond resulting in a red-shift of the CO stretching frequency. This problem is not specific to the CO adsorption in zeolites: similar effects have been observed for CO adsorbed on transition metals. In this case, Kresse et al.²² have demonstrated that the adsorption behavior can be corrected by a molecular GGA+U method modifying the HOMO–LUMO gap by an on-site interaction added to the DFT Hamiltonian, and this is the approach suitable for metals. For insulating or molecular substrates, hybrid functionals mixing Hartree–Fock (HF) and DFT exchange can be used instead; the admixture of HF exchange increases the HOMO–LUMO gap and leads to an improved description of the CO interaction with the adsorption site.

Fortunately, the error in the CO stretching frequencies introduced by the DFT description can be corrected using a scaling method based on the $\omega_{\text{CO}}[\text{CCSD(T)}]/r_{\text{CO}}[\text{DFT}]$ correlation.^{11,19} Coupled cluster calculations are performed for small carbonyl molecules. As high-level quantum-chemical methods such as CCSD(T) correctly describe the HOMO–LUMO separation in CO, they also correctly predict the blue-shift of the stretching frequency. The CCSD(T) CO frequencies determined for these model systems may be used to estimate the

CO stretching frequencies in the metal–zeolite system by using a linear correlation between the CO bond length and the CO stretching frequency. A linear correlation between the CO bond length and the CO stretching frequency was pointed out by Ramprasad et al.,¹² and it is crucial for our approach. The correlation between the coupled clusters²³ (CCSD(T)) CO frequency and the CO equilibrium distance at the DFT level was firmly established.^{11,19} The problem of calculating the CO stretching frequencies at a highly correlated ab initio level is thus reduced to calculations of the CO equilibrium distances at the DFT level. Therefore, the size and topology of the model used for the representation of the zeolite framework remains the only obstacle in precise calculations of the CO stretching frequency for CO adsorbed on Cu⁺/zeolite systems.

The $\omega_{\text{CO}}/r_{\text{CO}}$ scaling method¹⁹ was used together with a combined quantum chemical/interatomic potential function (QM-pot)^{24,25} description of the high-silica Cu⁺/MFI zeolite, and the site-specific CO stretching frequencies were estimated with error less than 5 cm^{–1} from the experiment.¹¹ The potential drawback of this approach is the finite size (several tens of T atoms) of the inner part in the QM-pot description of the MFI zeolite and the fact that different definitions of the inner part are used for various Cu⁺ sites in zeolites. In principle, the CO stretching frequencies can be calculated using even larger definition of the inner part in QM-pot scheme than used in ref 11. The best way to test the convergence of the QM-pot model with respect to the size of the inner part treated quantum-mechanically, however, is to compare the QM-pot results with the periodic DFT calculations. The computational demands of periodic DFT methods depend on the volume of the unit cell. Due to the large volume of the MFI unit cell, the periodic DFT calculations with sufficiently flexible basis set are currently computationally prohibitive. Thus, high silica zeolites with smaller unit cells are more convenient for comparison of QM-pot and periodic DFT approaches.

Recently, IR spectra of the CO/Cu⁺/FER system (Si/Al ratio = 8, complete Cu⁺ ion exchange) were reported by Palomino et al.²⁶ At low CO equilibrium pressure, the spectrum shows a single absorption band at 2157 cm^{–1} with a half-width of $d_{1/2}$ = 11 cm^{–1}. This band was assigned to a monocarbonyl Cu⁺–CO species in agreement with previous experimental data.³ In this paper, we compare the performance of periodic DFT and QM-pot models combined with the $\omega_{\text{CO}}/r_{\text{CO}}$ scaling method for the description of CO stretching dynamics in the CO/Cu⁺/FER system. The aim of this work is 3-fold: (i) verify accuracy of the $\omega_{\text{CO}}/r_{\text{CO}}$ scaling method for calculations of the CO stretching frequencies in various zeolite structures, (ii) use of the $\omega_{\text{CO}}/r_{\text{CO}}$ scaling with the periodic DFT model, and (iii) check the convergence of the QM-pot models with respect to the inner part size. It should be pointed out that the applicability of the $\omega_{\text{CO}}/r_{\text{CO}}$ scaling method in combination with periodic DFT calculations is not obvious since the $\omega_{\text{CO}}/r_{\text{CO}}$ scaling method relies on very precise calculations of the CO bond length.

2. Calculations

The calculations of the CO stretching frequencies using the $\omega_{\text{CO}} - r_{\text{CO}}$ scaling method is relatively straightforward.

The equilibrium CO distances and corresponding harmonic frequencies are calculated for a set of small model molecules at DFT and CCSD(T) levels. The $\omega_{\text{CO}} - r_{\text{CO}}$ scaling parameters are obtained by fitting the linear dependence of CCSD(T) harmonic frequencies and DFT equilibrium distances

$$\omega_{\text{CO}}[\text{CCSD(T)}] = ar_{\text{CO}}[\text{DFT}] + b \quad (1)$$

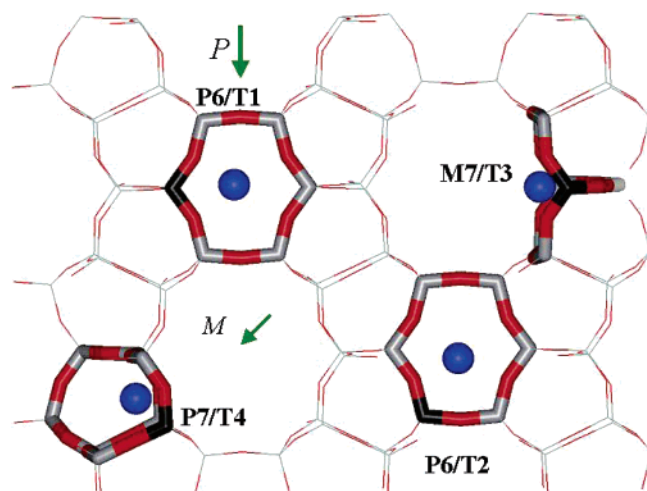


Figure 1. Cu^+ sites in FER. The direction of main (M) and perpendicular (P) channels is shown by arrows. P6/T1 and P6/T2 are sites on the wall of the perpendicular channel, P7/T4 site is on the wall of perpendicular channel close to the channel intersection, and M7/T3 site is on the wall of the main channel. Framework Al atoms are depicted in black.

The scaled harmonic frequencies obtained from eq 1 for CO adsorbed on a $\text{M}^+/\text{zeolite}$ tend to deviate from experiment in a systematic way. It reflects a more complex interaction of the CO molecule with molecular environment in zeolites. This can be fixed, however, by introducing a correction $\Delta\omega$ calculated as the difference of the scaled ω_{CO} from eq 1 and the CCSD(T) harmonic frequency for a simple zeolite model (typically $\text{Al}(\text{OH})_4\text{CuCO}$ (1T cluster) model possessing the basic features of cationic sites in the $\text{CO}/\text{Cu}^+/\text{zeolite}$ system).

The anharmonic correction $\Delta\nu$ is calculated using a two-dimensional (C–O, Cu–C) stretching Hamiltonian (ref 11).

Finally, the CO stretching frequency is evaluated as a sum of the following terms:

$$\nu_{\text{CO}} = \nu_{\text{CO}}[\text{DFT}] + b + \Delta\omega + \Delta\nu \quad (2)$$

In this paper, we use the 1T zeolite model for the $\Delta\omega$ correction and assume a constant anharmonic correction $\Delta\nu$ (-29 cm^{-1}) calculated previously for monocarbonyl species in various molecular environments.^{11,19} The resulting CO stretching frequencies obtained from eq 2 are expected to agree with corresponding experimental values to within few wavenumbers ($\sim 5 \text{ cm}^{-1}$).

2.1. Cu^+/FER Model. The single unit cell of Ferrierite contains 36 T atoms (Si or Al) and 72 O atoms. This cell was used in the periodic DFT calculations and a multiple of this unit cell (four or eight times) was used in the combined QM-pot calculations ($\text{T}_{144}\text{O}_{288}$ or $\text{T}_{288}\text{O}_{576}$, respectively). In all calculations, a single framework Si atom was replaced by an Al atom and the charge was compensated by a single Cu^+ cation. Calculations were carried out for each of four distinguishable framework T-positions (four distinguishable T-sites are calculated in the I_{mmm} space group, the numbering scheme of ref 27 is adopted).²⁸ The Cu^+ ion was placed to the most stable site for each location of the framework Al atom.²⁹ Therefore, the interaction of CO with P6/T1 (Cu^+ at P6 site and Al at T1 position), P6/T2, M7/T3, and P7/T4 Cu^+ sites (Figure 1) was investigated. The periodic boundary conditions were applied and the geometries were optimized without any symmetry constraints (P1 symmetry).

2.2. Periodic DFT Model of $\text{CO}/\text{Cu}^+/\text{FER}$. Periodic ab initio calculations were performed using the VASP code.^{30–33}

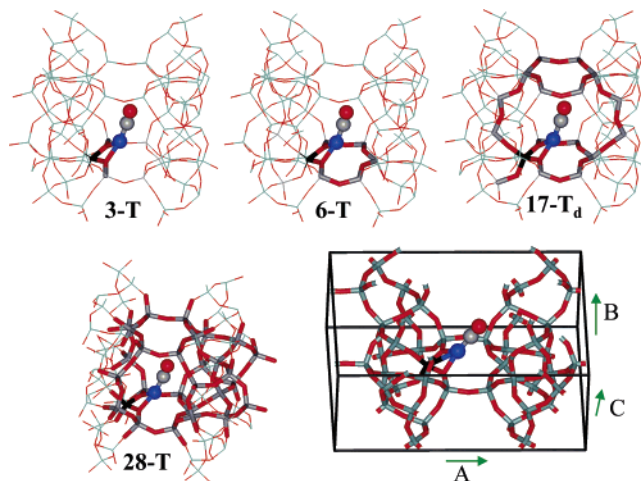


Figure 2. $\text{CO}/\text{Cu}^+/\text{FER}$ models. The QM-pot models using 3-T, 6-T, 17-T_d, and 28-T inner parts (framework T-atoms from the inner part depicted in tube mode) and unit cell used in periodic DFT calculations.

The Kohn–Sham equations were solved variationally with a plane-wave basis set using the projector-augmented-wave (PAW) of Blöchl (ref 34) as recently adapted by Kresse and Joubert (ref 35). The Perdew and Wang (PW91)^{36,37} and Perdew–Burke–Erzenhofer (PBE)^{38,39} functionals were used together with the plane-wave basis set with the energy cutoff of 600 eV (unless stated otherwise). Brillouin-zone sampling was restricted to the gamma-point.

The equilibrium volume of the all-silica FER unit cell was fitted using the Murnaghan’s equation of state. The calculations with plane-wave basis set using 400, 500, and 600 eV energy cutoff show very small dependence of the fitted volume on the basis set. The unit cell obtained for the all-silica form with a 600 eV cutoff (cell parameters 19.1468, 14.3040, and 7.5763 Å, volume 2076.70 Å³) was used in all further calculations on $\text{CO}/\text{Cu}^+/\text{FER}$ and also in the calculations on a set of small molecules used for the evaluation of the $\omega_{\text{CO}} - r_{\text{CO}}$ correlation.

2.3. QM-Pot Model of $\text{CO}/\text{Cu}^+/\text{FER}$. Within the combined quantum mechanical/interatomic potential function (QM-pot) method^{24,25} the system is divided into two parts: the inner part, which includes Cu^+CO and framework atoms in its vicinity, is treated at the DFT level, and the outer part including all of the remaining atoms of the periodic cell where the interactions among the atoms are described at the computationally less expensive IPF level. The dangling bonds of the inner part were saturated by hydrogen atoms connected to framework oxygen atoms (OH termination). The inner part together with terminating H-atoms forms a cluster. Various sizes of the inner part (cluster) were used in the calculations, ranging from 1-T ($\text{COCuAlO}_4\text{H}_4$) to 31-T ($\text{COCuAlSi}_{30}\text{O}_{80}\text{H}_{34}$) cluster models (notation indicates the number of framework T-atoms in the cluster). Examples of cluster models used for the description of CO interaction with the P6/T1 site are depicted in Figure 2. Rather large inner part definitions were used for reliable calculations of the CO stretching frequencies. The size of the inner part depends on the particular position of the framework Al atom and on the Cu^+CO orientation within the zeolite. The interaction of both Cu^+ and CO with the framework must be described at the DFT level.

The DFT calculations with Gaussian type orbital (GTO) basis set were carried out employing the BLYP^{40,41} and PBE^{38,39} exchange–correlation functionals and valence–triple- ζ -plus-polarization function basis set, VTZP, for C and O atoms, valence–double- ζ -plus-polarization function basis set, VDZP,

TABLE 1: Parameters of the $\omega_{\text{CO}} - r_{\text{CO}}$ Correlation for CO/Cu⁺/Zeolite Systems^a

| basis sets | a/Å ⁻¹ cm ⁻¹ | b/cm ⁻¹ | $\Delta\omega^a/\text{cm}^{-1}$ |
|----------------------|------------------------------------|--------------------|---------------------------------|
| BLYP/GTO | -5683.8 | 8705.4 | -11 |
| PBE/GTO | -5764.3 | 8795.7 | -11 |
| PW91/600 single cell | -5742.0 | 8786.5 | -7 |
| PW91/600 double cell | -6056.7 | 9146.7 | -8 |
| PBE/600 single cell | -5720.1 | 8769.3 | -7 |
| PBE/600 double cell | -6038.9 | 9134.8 | -8 |

^a $\Delta\omega$ correction calculated from 1T model.

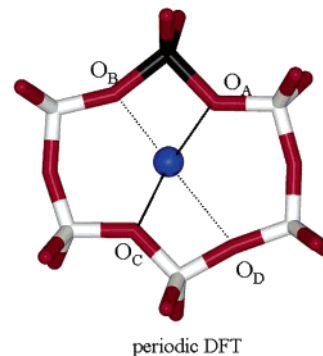
for Al, Si, and H atoms, and valence-triple- ζ basis set for Cu (“Basis set 2”, BS2).^{42,43} The resolution of identity (RI) approximation⁴⁴ was used. The (17s4p4d3f4g)/[7s4p2d3f2g], (12s6p5d1f1g)/[5s3p2d1f1g], (12s4p5d1f)/[5s3p2d1f], (9s3p3d1f)/[7s3p3d1f], (9s3p3d1f)/[7s3p3d1f], (4s2p1d)/[3s2p1d] auxiliary basis sets^{45–47} were used in RI calculations for Cu, Si, Al, C, O, and H atoms, respectively. The interactions between atoms outside the inner part (outer part) and cross-interactions between atoms from the inner and outer parts were treated at the interatomic potential function (IPF) level, employing core–shell model potentials.^{48,49} The interaction between the CO molecule and zeolite framework was treated with the Lennard-Jones potential with parameters derived from the universal force field.⁵⁰ Charges 0.3565 and -0.3565 were placed on the C and O atom of the CO molecule, respectively.¹¹ The calculations were performed with the QM-pot²⁴ program, which makes use of the TurboDFT⁵¹ and GULP⁵² programs for DFT and IPF calculations, respectively.

2.4. $\omega_{\text{CO}} - r_{\text{CO}}$ Correlation. The parameters a and b (eq 1) were evaluated from the calculations on the set of small molecules including Cu⁺CO, H₂O...Cu⁺CO, (H₂O)₂...Cu⁺CO, F⁻...Cu⁺CO, and (F⁻)₂...Cu⁺CO species. The geometries of these species were fully optimized at the DFT and CCSD(T) levels using the C_{2v} symmetry constraints, except the Cu⁺CO and F⁻...Cu⁺CO species for which the $C_{\infty v}$ symmetry was imposed. The CCSD(T) calculations were carried out with the correlation consistent valence-quadruple- ζ basis set with polarization functions^{53,54} (cc-pVQZ) for H, O, C, and F atoms and with the effective-core relativistic pseudopotential (replacing 10 inner electrons) and valence (8s7p6d2f1g)/[6s5p3d2f1g] basis sets, denoted ECP-2f1g, for Cu atom^{55–57} (this combination of basis sets will be denoted as “Basis set 1”, BS1). The CCSD(T) calculations were carried out with the Molpro program suite.^{58–60} The DFT calculations with GTO basis set were carried out with BLYP and PBE functionals and BS2 basis set defined above. The DFT calculations with plane-wave basis set were carried out using PBE and PW91 functionals and the energy cutoff 600 eV. The “super-cell” of the FER unit cell size (see above) was used. Parameters a and b obtained for various exchange-correlation functionals and basis sets are given in Table 1.

2.5. $\Delta\omega$ Correction. The geometry of the Al(OH)₄⁻...Cu⁺CO complex was fully optimized using the C_{2v} symmetry constraints for various DFT/BS combinations used in the calculations on CO/Cu⁺/FER. Only three geometry parameters (Al–Cu, Cu–C, and C–O distances) were varied in the CCSD(T) optimization for the Al(OH)₄⁻...Cu⁺CO model, and all other parameters were fixed at the corresponding BLYP/BS2 equilibrium values. The CCSD(T) frequencies were evaluated using the two-dimensional (Cu–C, C–O) stretching Hamiltonian (see ref 11 for more details). Due to the relatively large size of the Al(OH)₄⁻...Cu⁺CO model, the calculations at the periodic DFT level were repeated for double-supercell (considering all three possible cell enlargements). Only the cell size enlargement along the shortest cell side was found to be important. Therefore, the

TABLE 2: Cu⁺ Coordination to Framework Oxygen Atoms of the Six-Membered Ring on the Wall of the Perpendicular Channel (P6/T1 Site)^a

| functional | QM-pot | | | | periodic DFT |
|---------------------------|-----------|------|------|------|--------------|
| | 6-T/B3LYP | 6-T | 17-T | 28-T | |
| $r(\text{Cu}-\text{O}_A)$ | 2.06 | 2.03 | 2.00 | 2.02 | 1.95 |
| $r(\text{Cu}-\text{O}_B)$ | 2.14 | 2.17 | 2.14 | 2.15 | 2.27 |
| $r(\text{Cu}-\text{O}_C)$ | 2.12 | 2.07 | 2.04 | 2.05 | 2.00 |
| $r(\text{Cu}-\text{O}_D)$ | 2.44 | 2.48 | 2.40 | 2.47 | 2.79 |

^a Distances in Å. ^a Calculations carried out with PBE functional unless stated otherwise.**Figure 3.** Cu⁺ site on the wall of perpendicular channel (P6/T1 site).

$\omega_{\text{CO}} - r_{\text{CO}}$ correlation and $\Delta\omega$ correction were recalculated with double-cell (19.1468, 14.3040, and 15.1526 Å). The $\Delta\omega$ corrections are summarized in Table 1. Note that $\Delta\omega$ depends on the basis set used, however, it does not depend on the exchange-correlation functional.

3. Results

The results obtained with periodic DFT and combined QM-pot models are compared and the differences are analyzed. The convergence of the QM-pot models with respect to the size of the inner part was checked by comparison with the full periodic approach. The detail analysis of the inner (quantum mechanical) part size convergence is presented for the P6/T1 Cu⁺ site located on top of the six-membered ring on the wall of the perpendicular channel (Al atom in T1 position, Figure 1). The QM-pot calculations with the inner part described with 1-T, 3-T, 6-T, 8-T_d, 17-T_d, and 28-T clusters (see Figure 2) were performed.

3.1. QM-Pot vs Periodic DFT Models. 3.1.1. Cu⁺ Coordination. In agreement with a previous QM-pot study,²⁹ two types of Cu⁺ sites were found at the periodic DFT level: sites on the channel wall (type I) and sites on the channel intersection (type II). Sites on the channel wall are found energetically more stable than sites on the channel intersection when the framework Al atom is placed in the T1, T3, or T4 position. However, an intersection site energetically below channel wall site is found at the periodic DFT level when Al is at T2 position, contrary to the results of previous QM-pot study.²⁹ This discrepancy is due to the differences between periodic DFT and QM-pot models,⁶¹ it does not result from the use of different functionals in QM-pot and periodic DFT calculations.

A detailed comparison of Cu⁺ coordination obtained at the periodic DFT and QM-pot levels is presented in Table 2 for the P6/T1 site. Geometrical parameters are defined in Figure 3. The preference of Cu⁺ for a linear two-coordinated structure is apparent at the periodic DFT level: two strong bonds are formed to the O_A and O_C framework oxygen atoms with an almost straight O_A–Cu–O_C angle (168.5°). The Cu⁺ coordination is

TABLE 3: Comparison of Harmonic CO Stretching Frequencies and CO Adsorption Energies Obtained at the QM-Pot and Periodic DFT Levels^a

| | | $r(\text{CO})^b$ | $\omega(\text{CO})^c$ | $\nu(\text{CO})^{c,d}$ | E_{ads}^e |
|---------------------------|-----------------------------|------------------|-----------------------|------------------------|--------------------|
| QM-pot ^f | | | | | |
| BLYP/PBE | 1-T | 1.1487 | 2177 | 2137 | −50.6 |
| | 3-T | 1.1478 | 2182 | 2142 | −51.3 |
| | 6-T | 1.1484 | 2178 | 2138 | −35.5 |
| | 6-T [no q(CO)] ^h | | | | −38.7 |
| | 8-T _d | 1.1478 | 2182 | 2142 | −35.7 |
| | 16T/8 UC | 1.1449 | 2198 | 2158 | |
| | 17T _d /8 UC | 1.1447 | 2199 | 2159 | −36.5 |
| | 28 T/8 UC | 1.1458 | 2193 | 2153 | −34.0 |
| Periodic DFT ^g | | | | | |
| PBE | 600 eV | 1.1500 | 2191 | 2154 | −33.6 |
| PBE | 450 eV | | | | −34.5 |
| PBE | 300 eV | | | | −36.5 |
| PW91 | 600 eV | 1.1486 | 2191 | 2154 | |

^a Calculated for P6 site, Al at T1 position. ^b In Å. ^c In cm^{−1}. ^d Calculated from eq 2, $\Delta\nu = -29 \text{ cm}^{-1}$ used for all models. ^e In kcal/mol. ^f Inner part size defined; $r(\text{CO})$ and $\nu(\text{CO})$ calculated with BLYP functional, E_{ads} calculated with PBE functional. ^g Density functional and plane-wave cutoff specified. ^h Electrostatic contribution to the interaction of CO with framework atoms outside the inner part is not considered.

further stabilized by the interaction of Cu⁺ with the framework O_B oxygen atom. Qualitatively, the same structure is found also at the QM-pot level, however, the difference between the two short bonds (to O_A and O_C) and the longer bonds (to O_B and O_D) is not as large as at the periodic DFT level. It appears that the Cu⁺ coordination at the P6/T1 site is accompanied by changes in the geometry of framework atoms in the second and higher coordination shells. These changes in the framework geometry at larger distances from the Cu⁺ ion are not properly reflected when IPF potentials are used for the description of atoms in outer part of QM-pot scheme.

The structures obtained with B3LYP and PBE functionals (6-T model) are similar; however, the preference for a linear Cu⁺ coordination is less apparent at the B3LYP level (the Cu⁺ distances to O_B and O_C oxygen atoms are almost the same). A preference of Cu⁺ for a linear coordination was also found for all other Cu⁺ sites investigated at the periodic DFT level: among the two closest neighbors of Cu⁺ one is a framework oxygen atom belonging to the AlO₄ tetrahedron and one oxygen atom of a SiO₄ tetrahedron.

3.1.2. CO Adsorption Energies. Adsorption energies were calculated with the PBE functional in both periodic DFT and QM-pot models. Results are summarized in Table 3. Upon interaction with CO, the coordination of Cu⁺ with the framework oxygen atoms is changed: the Cu⁺ ion is now coordinated to just two oxygen atoms of AlO₄ tetrahedron (Figure 2), as already described in ref 14. Adsorption energies calculated at the QM-pot level using a small inner part (represented by 1-T or 3-T clusters) are significantly overestimated compared to the results obtained with a larger definition of the inner part or with the periodic DFT model. This is due to the fact that 1-T and 3-T clusters cannot account properly for the interaction of the bare Cu⁺ ion with the six-membered ring (P6 site, Figure 1). When 6-T or larger clusters are used for the representation of the inner part of the QM-pot model (6-T, 8-T_d, 17-T_d, and 28-T clusters) the CO adsorption energies do not depend on the size of the model. When 6-T or 8-T_d cluster models are used, the charges on C and O atoms of CO must be used in order to obtain reliable adsorption energies. Calculations at the QM-pot level using a 6-T cluster with and without charges on CO give adsorption energies of −35.5 and −38.7 kcal/mol, respectively. When a

large inner part definition is used (17-T_d and 28-T models), the adsorption energies do not depend on the charge on the CO ligand. The BSSE (calculated at QM-pot level using 6-T cluster for inner part) is 3.3 kcal/mol, thus, the CO adsorption energy calculated at the QM-pot level using the PBE functional and a large (28-T) inner part is −30.7 kcal/mol.⁶²

The interaction energies at the periodic DFT level were obtained as the difference between the energy of the CO/Cu⁺/FER system and the energies of a bare CO molecule and Cu⁺/FER, each of them calculated with the same unit cell and the same basis set (600 eV cutoff). Therefore, the adsorption energy calculated at the periodic DFT level is not influenced by a basis set superposition error. To check the quality of the basis set used in periodic DFT calculations the CO adsorption energies were calculated also using 300 and 450 eV cutoff energy. The adsorption energy gets smaller with the increasing size of the basis set. From Table 3, we conclude that the CO interaction energy calculated with periodic model and PBE functional is smaller than −33.6 kcal/mol (by 1–2 kcal/mol). Thus, the CO adsorption energies calculated at the QM-pot level are in very good agreement (within 2 kcal/mol) with the results obtained with the periodic DFT model. It should be noted, however, that DFT calculations employing LDA or GGA functionals lead to a substantial overestimation of the adsorption energy compared to experiment. This tendency is particularly pronounced for CO adsorption on metal cations due to the underestimation of the HOMO–LUMO gap, as discussed in the Introduction. The good convergence of the periodic DFT and QM-pot calculations justifies another approach based on hybrid functionals used for a relatively small inner part of combined model. Based on the results summarized in Table 3 we expect that the QM-pot method with a relatively small inner part (6-T), NBO charges on CO, and B3LYP functional should provide reliable CO adsorption energies for Cu⁺/zeolites. Indeed, at the QM-pot level (6-T inner part, B3LYP functional, NBO charges on CO, BSSE, and ZPE corrections) the CO adsorption energy on P6/T1 site is −18.1 kcal/mol in good agreement with experimental data (−20.5 kcal/mol).⁶³

3.1.3. CO Stretching Frequencies. The CO stretching frequencies for CO adsorbed at the P6/T1 site (see. Figure 2) calculated from the $\omega_{\text{CO}} - r_{\text{CO}}$ correlation (eqs 1 and 2) do not depend on the choice of the exchange-correlation functional (Table 3). Frequencies calculated with the periodic DFT model and with the QM-pot model employing a large inner part (28-T cluster) are in excellent agreement (2154 and 2153 cm^{−1}, respectively). The $\Delta\omega$ corrections (accounting for the difference in the local environments of CO in the carbonyl molecules used in the CCSD(T) calculations of ω_{CO} and in the Cu⁺/zeolite) corrects the frequency by about −8 and −11 cm^{−1}, for periodic DFT and QM-pot, respectively. However, the QM-pot results depend on the definition of the inner part. Although calculations with a rather large inner part (28-T) give reliable stretching frequencies, the results obtained with smaller inner parts are less satisfactory. Based on the inner part size of the QM-pot scheme, these models can be divided into three groups: (i) Small models describing at the DFT level only the interaction of the Cu⁺CO complex with the zeolite framework on the “copper-side” of the zeolite channel (1-T, 3-T, 6-T, 8-T_d models). The interaction of CO with the framework atoms on the “opposite-side” of the channel is treated entirely at the interatomic potential function (IPF) level. (ii) Medium size models (16-T and 17-T_d) describing at the DFT level the interaction of the Cu⁺CO complex on the copper-side of the channel and also the interaction with the framework atoms on the opposite side of

TABLE 4: r_{CO} Bond Lengths (in Å) and CO Stretching Frequencies (in cm^{-1}) Calculated for Individual Cu^+ Sites in FER Using Periodic DFT and QM-Pot Models

| | | | Cu^+ site/framework Al position ^a | | | |
|---------------------------|---------------------|-------------------|---|--------|--------|----------------|
| | | | P6/T1 | P6/T2 | M7/T3 | P7/T4 |
| periodic DFT ^b | | r_{CO} | 1.1486 | 1.1482 | 1.1483 | 1.1483 |
| | | ν_{CO} | 2154 | 2157 | 2156 | 2156 |
| QM-pot ^c | large ^f | r_{CO} | 1.1458 | 1.1437 | 1.1448 | 1.1449 |
| | | ν_{CO} | 2153 | 2165 | 2159 | 2158 |
| | medium ^d | r_{CO} | 1.1449 | 1.1436 | 1.1440 | - ^e |
| | | ν_{CO} | 2158 | 2166 | 2163 | - ^e |

^a Cu^+ sites defined in Figure 1. ^b PW91 exchange-correlation functional used. ^c BLYP functional used. ^d Inner parts consisting of 16, 16, and 19 T-atoms were used for P6/T1, P6/T2, and M7/T3 sites, respectively. ^e We were not able to define any suitable medium size cluster for description of this site. ^f Inner parts consisting of 28, 31, 22, and 26 T-atoms were used for P6/T1, P6/T2, M7/T3, and P7/T4 sites, respectively.

the channel (see Figure 2). (iii) A large model (28-T) treating at the DFT level most of the interaction between the framework and CO (framework O atoms within 7 Å from oxygen of CO molecule, Figure 2). The CO stretching frequencies calculated with the small models are in the range 2137–2142 cm^{-1} , about 10–15 cm^{-1} below the results obtained with the periodic DFT model. Calculations with the medium size model (16-T, 17-T_d) show that the repulsive interaction of CO with the close framework oxygen atoms from the opposite side of the channel results in a blue-shift of $\nu(\text{CO})$ (about 15–20 cm^{-1}). The interaction of CO with additional oxygen atoms included in the large 28-T model somewhat mediates the repulsive interaction of CO with the close oxygen atoms on the channel wall surface. As a consequence, the enlargement of the model from 16-T to 28-T results in the small decrease of calculated CO stretching frequencies (about 5 cm^{-1}). The variation of r_{CO} and ν_{CO} with the size of the model does not necessarily reflect a physical effect such as an increased interaction of CO with the inner wall of the zeolite cavity but depends in a delicate way on the OH termination of the inner part and the interaction between the inner and outer parts (see Discussion section for more details).

3.2. CO Stretching Frequencies for the CO– Cu^+ /Ferrierite System. The CO stretching dynamics was investigated for four Cu^+ sites in Cu^+ /FER. Calculated r_{CO} bond lengths and CO stretching frequencies based on eq 2 are summarized in Table 4. The CO frequencies calculated at the periodic DFT level (PW91 functional) are in the range 2154–2157 cm^{-1} , in excellent agreement with experimental data (peak maximum at 2157 cm^{-1} , half-width 11.1 cm^{-1}).²⁶ The frequencies calculated at the QM-pot level (BLYP functional) employing large inner parts are in very good agreement with the periodic DFT results when Cu^+ is placed in P6/T1, M7/T3, and P7/T4 sites (the difference between the QM-pot and periodic DFT frequencies is not larger than 3 cm^{-1}). However, a somewhat higher frequency was found for the P6/T2 site at the QM-pot level compared to the periodic DFT calculations (2166 and 2156 cm^{-1} , respectively). Further enlargement of the model (beyond 31-T model) on the opposite side of the channel does not improve the results. The analysis of structures obtained with the QM-pot and periodic DFT models shows that the problem of the QM-pot model is not due to the description of the CO interaction with the channel wall (as is the case of small or medium-size models). Instead, the problem is in the description of the Cu^+ interaction with the zeolite framework. It appears that the Cu^+ coordination at this site is slightly different according to periodic DFT and QM-pot models. Upon CO adsorption, the Cu^+ ion is coordinated to two oxygen atoms of the AlO_4 tetrahedron at the periodic DFT level, whereas at the QM-pot level, the Cu^+ ion is coordinated to only one atom of AlO_4 . The differences in Cu^+ coordination and associated

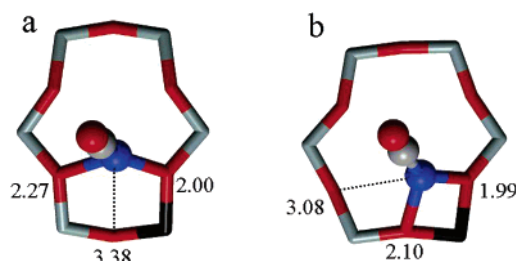


Figure 4. The CO adsorption complex on P6/T2 site optimized at QM-pot (a) and periodic DFT (b) levels. Framework Al atom depicted in black. Cu–O bond lengths in Å.

differences in the geometry of the six-membered ring are depicted in Figure 4. As a consequence, charge transfer from the zeolite to Cu^+ is smaller at the QM-pot geometry than at the periodic DFT structure. The larger electron density of the Cu^+ ion coordinated to two oxygen atoms of the AlO_4 tetrahedron results in a larger electron back-donation to CO and, thus, to a lower CO stretching frequency at the periodic DFT level than at the QM-pot level for this particular Cu^+ site.

4. Discussion

Adsorption energies calculated for CO at the P6/T1 site at the QM-pot level (employing 6-T or larger inner part definition) and at the periodic DFT level are in good agreement. It should be noted that further improvement of the basis set used in the periodic DFT model will result in a small decrease of the interaction energy, and thus even a better agreement between two rather different models can be expected. Interaction energies calculated at the QM-pot level using a large inner part (28-T) do not depend on the long-range (beyond the boundary of the inner part) electrostatic interactions between partial charges on CO and on the framework atoms. Even when the small inner part is used within the QM-pot scheme (as small as 6-T), the interaction energy can be reliably calculated when partial charges on CO are defined properly. The interaction energy calculated with this model (–32.2 kcal/mol upon BSSE correction) is in very good agreement with the result of the periodic DFT model. This is an important verification of the suitability of NBO charges used on CO in this study since the definition of the partial charges used in the IPF model is always problematic and not easy to verify. The electrostatic interaction of CO with the zeolite channel wall is 3.2 kcal/mol and repulsive. This repulsion is almost entirely due to the CO interaction with framework oxygen atoms on the surface of the channel wall. At this point, it is important to mention that all DFT calculations (periodic or QM-pot) overestimate the adsorption energy. However, the analysis of the convergence of the QM-pot calculations justifies the calculation of adsorption energies using hybrid functionals and relatively small inner part of the QM-

pot model. The role of the HF-exchange contribution is to correct the underestimation of the HOMO–LUMO gap of CO that is characteristic for LDA and GGA functionals.

The CO adsorption energy calculated for the P6/T1 site is -18.1 kcal/mol in good agreement with experimental data (-20.5 kcal/mol)⁶³ obtained from the analysis of TPD curves. To the best of our knowledge, there are no calorimetric data available for the CO/Cu⁺/FER system. Therefore, we compare our results with calorimetric data obtained for the CO/Cu⁺/MFI system. Kumashiro et al. found two types of Cu⁺ sites characterized by adsorption energies 29 and 24 kcal/mol.⁶⁴ Bolis et al. observed that the differential heat of adsorption continuously decreased from 31 to 10 kcal/mol.⁶⁵ It was concluded that there is only a fraction (about one-third) of Cu⁺ sites with CO adsorption energies higher than 24 kcal/mol. It has been shown previously that CO interaction energies differ for intersection sites and for channel wall sites.¹⁴ The CO adsorption on Cu⁺ at the P6/T1 site in FER is about 10 kcal/mol smaller than CO adsorption energy on intersection site. Therefore, the interaction energy of CO on channel wall site P6/T1 is not in contradiction with available calorimetric data; however, a direct comparison cannot be done.

Calculations of the vibrational frequencies of a probe molecule with spectroscopic accuracy for large complex system are important for interpretation of experimental spectra at the atomic scale level. The most common approaches used for calculations of vibrational dynamics fail to reproduce the stretching frequency of CO adsorbed on a Cu⁺/zeolite. The vibrational frequencies are typically obtained from normal-mode analysis. If analytic second derivatives are not available, this can be achieved by the finite differences method. The CO stretching frequencies were calculated by finite difference method and periodic DFT model employing PW91, PBE, and RPBE functional. Hessians of various dimensions were considered. Stretching frequencies obtained for the CO molecule adsorbed on the P6/T1 site were calculated using a dynamical matrix approximated by three atoms (Cu, C, and O). ν_{CO} calculated with PW91 and PBE functionals (2055 and 2053 cm⁻¹, respectively) are about 100 cm⁻¹ below the experimental value. Contrary to experimental observation²⁶ calculated ν_{CO} are about 15 cm⁻¹ red-shifted with respect to the CO frequency of the gas-phase molecule calculated at the same level of theory. The prediction of a red-shift corresponds to the overestimation of the adsorption energy; both the overbinding between CO and Cu⁺ and the reduction of the strength of the intramolecular C–O bond are due to a too strong back-donation from the Cu⁺-d-states to the antibonding $2\pi^*$ orbitals of CO. The M⁺(d)–CO- ($2\pi^*$) interaction is peculiar to transition metal cations and to Cu⁺ with occupied d-states close to the Fermi energy. In alkali metal cations (Na⁺), polyvalent metal ions (Al³⁺, Zn²⁺), and at Brönsted sites (H⁺), no back-donation into the $2\pi^*$ orbitals can occur because of the absence of occupied near Fermi-edge orbitals. In Ag⁺, the d-levels are moved far enough below the Fermi level to suppress the back-donation even for low energy $2\pi^*$ level predicted at the DFT level. To convert the red-shift produced by DFT calculations into a blue-shift requires a high-level quantum chemical approach correcting the HOMO–LUMO gap. However, high-level (post HF) calculations are not feasible for complex periodic models of zeolites.

The alternative is to use semiempirical scaling procedures to improve agreement of calculated frequencies obtained from normal-mode analysis with experimental fundamentals.^{15,66} However, such a scaling alone cannot change the wrong sign of CO frequency shift upon adsorption. It has been shown

recently¹¹ that accurate CO stretching frequencies can be derived using the $\omega_{\text{CO}}/r_{\text{CO}}$ correlation. In principle, a $\omega_{\text{CO}}[\text{CCSD(T)}]/\omega_{\text{CO}}[\text{DFT}]$ correlation could be used instead of the $\omega_{\text{CO}}/r_{\text{CO}}$ correlation and a good agreement between the experimental and calculated frequencies is expected when this correlation is applied on the CO frequencies obtained by finite differences method. However, within the $\omega_{\text{CO}} - r_{\text{CO}}$ correlation, only the CO bond length at the minimum energy structure is required, without the need to evaluate the second derivatives of the energy with respect to the atomic coordinates. Therefore, the $\omega_{\text{CO}}/r_{\text{CO}}$ correlation method represents a much simpler access to precise frequency calculations than a $\omega_{\text{CO}}[\text{CCSD(T)}]/\omega_{\text{CO}}[\text{DFT}]$ scaling method.

A certain importance of long-range interactions on the CO stretching dynamics can be understood from the data presented in Table 3. A very good agreement between CO frequencies calculated using the $\omega_{\text{CO}}/r_{\text{CO}}$ correlation at the periodic DFT level and those calculated at the QM-pot level employing a large inner part (with and without charges on CO) clearly indicates that the effect of the Madelung potential on the CO vibrational dynamics is marginal. The same conclusion was drawn recently for CO/Cu⁺/MFI system.¹¹ Frequencies calculated at the QM-pot level and medium-size inner part (16-T and 17-T_d) are about 5 cm⁻¹ larger than those calculated at QM-pot level employing a larger inner part. With a large 28-T model all framework oxygen atoms (O_f) within 7 Å from the oxygen atom of CO (O_{co}) are included in the inner part of the combined model (except one). All O_f atoms within 6 Å of O_{co} (except three) neighbor two Si atoms (Si–O–Si environment). This appears to be important since the O_{co}...O_f interaction is different for Si–O–H environment (cluster terminating link atoms on the inner part boundaries) than for Si–O–Si environment. Simple model calculations using Al(OH)₄CuCO...H–O_f–SiH₃ and Al(OH)₄CuCO...SiH₃–O_f–SiH₃ models (linear Al–Cu–C–O...O_f arrangement) show that at distances $r(\text{O}_{\text{co}}\text{O}_f) = 4$ and 5 Å the H–O_f–Si model gives 1.5 and 0.8 cm⁻¹ larger CO frequencies than Si–O_f–Si model, respectively. This is probably the reason for small deficiency of the QM-pot model with medium-size inner part in the description of the CO vibrational dynamics: within 5 Å from O_{co} there are two O_f atoms that are not included in the 17-T_d model at all and four O_f atoms on the cluster boundaries described as Si–O–H.

5. Conclusions

Two considerably different models (periodic DFT and combined quantum mechanics/interatomic potential function models) were used to describe the interaction of CO with the Cu⁺ sites in FER. When a sufficiently large inner part (cluster) is used the QM-pot approach results are in good agreement with those obtained at the periodic DFT level. The size of the inner part depends on investigated properties. Although the CO interaction energy with Cu⁺/FER can be reliably obtained with only six TO₄ tetrahedra in the inner part and hybrid B3LYP functional, the calculations of CO stretching frequencies require a significantly larger model. Both, periodic DFT and QM-pot models are suitable for the description of the CO/Cu⁺/FER system giving the same adsorption energies and the same CO stretching frequencies, in excellent agreement with experiment. We believe that this is important conclusion since different approximations are used in each of the models.

The effects of the zeolite framework on the CO interaction with the Cu⁺ ion were analyzed. Upon the interaction with CO the Cu⁺ ion reduces its coordination with the zeolite framework staying coordinated to only two framework oxygen atoms of the single AlO₄ tetrahedron.

Periodic DFT and QM-pot calculations using GGA exchange-correlation functionals (e.g., BLYP, PBE, and PW91) produce too large adsorption energies and too low CO stretching frequencies. Both effects are due to overestimated Cu⁺(d)–CO(2 π^*) back-donation which is a consequence of underestimated HOMO–LUMO gap. On the contrary, CO adsorption energies calculated with hybrid B3LYP functional are in good agreement with experimental data.

A drawback of the GGA functionals (overestimated Cu⁺(d)–CO(2 π^*) back-donation) can be overcome in calculations of CO stretching frequencies. The CO stretching frequency can be reliably obtained using a $\omega_{\text{CO}}/r_{\text{CO}}$ correlation method. The CO stretching frequencies calculated for various Cu⁺ sites in FER at the periodic DFT level are in the narrow range 2154–2157 cm^{−1}, in excellent agreement with the experimental spectra (band at 2157 cm^{−1}, half-width 11.1 cm^{−1}).^{3,26} Frequencies calculated at the QM-pot level (using large inner part) are in the range 2153–2165 cm^{−1}, also in good agreement with the experimental data. The CO stretching frequencies are not site-specific in the CO/Cu⁺/FER system.

Acknowledgment. Work in Prague was supported by research Project Z4 055 905 and by Grant LC512 from Czech Ministry of Education. M.S. thanks the Marie Curie Training Site “Atomic Scale Computational Materials Science” for support and hospitality. Work in Vienna was supported by the Austrian Science Funds under project No. P17020. We thank Marek Sierka and Joachim Sauer for providing the QM-pot code and Julian Gale for the GULP code.

References and Notes

- (1) Hadjiivanov, K. I.; Vayssilov, G. N. Characterization of oxide surfaces and zeolites by carbon monoxide as an IR probe molecule. *Adv. Catal.* **2002**, *47*, 307.
- (2) Iwamoto, M.; Furukawa, H.; Mine, Y.; Uemura, F.; Mikuriya, S.; Kagawa, S. *J. Chem. Soc., Chem. Commun.* **1986**, 1272.
- (3) Iwamoto, M.; Hoshino, Y. *Inorg. Chem.* **1996**, *35*, 6918.
- (4) Lamberti, C.; Bordiga, S.; Salvalaggio, M.; Spoto, G.; Zecchina, A.; Geobaldo, F.; Vlaic, G.; Bellatreccia, M. *J. Phys. Chem. B* **1997**, *101*, 344.
- (5) Lamberti, C.; Palomino, G. T.; Bordiga, S.; Berlier, G.; D’Acapito, F.; Zecchina, A. *Angew. Chem.-Int. Ed.* **2000**, *39*, 2138.
- (6) Zecchina, A.; Bordiga, S.; Palomino, G. T.; Scarano, D.; Lamberti, C.; Salvalaggio, M. *J. Phys. Chem. B* **1999**, *103*, 3833.
- (7) Bolis, V.; Barbaglia, A.; Bordiga, S.; Lamberti, C.; Zecchina, A. *J. Phys. Chem. B* **2004**, *108*, 9970.
- (8) Goldman, A. S.; Krogh-Jespersen, K. *J. Am. Chem. Soc.* **1996**, *118*, 12159.
- (9) Lupinetti, A. J.; Strauss, S. H.; Frenking, G. *Prog. Inorg. Chem.* **2001**, *49*, 1.
- (10) Treesukol, P.; Limtrakul, J.; Truong, T. N. *J. Phys. Chem. B* **2001**, *105*, 2421.
- (11) Bludský, O.; Silhan, M.; Nachtigallova, D.; Nachtigall, P. *J. Phys. Chem. A* **2003**, *107*, 10381.
- (12) Ramprasad, R.; Schneider, W. F.; Hass, K. C.; Adams, J. B. *J. Phys. Chem. B* **1997**, *101*, 1940.
- (13) Schneider, W. F.; Hass, K. C.; Ramprasad, R.; Adams, J. B. *J. Phys. Chem. B* **1998**, *102*, 3692.
- (14) Davidova, M.; Nachtigallova, D.; Bulanek, R.; Nachtigall, P. *J. Phys. Chem. B* **2003**, *107*, 2327.
- (15) Scott, A. P.; Radom, L. *J. Phys. Chem.* **1996**, *100*, 16502.
- (16) Benco, L.; Bucko, T.; Hafner, J.; Toulhoat, H. *J. Phys. Chem. B* **2004**, *108*, 13656.
- (17) Bucko, T.; Benco, L.; Hafner, H. *J. Phys. Chem. B* **2005**, submitted.
- (18) Benco, L.; Bucko, T.; Hafner, H. *J. Phys. Chem. B* **2005**, *109*, 7345.
- (19) Bludský, O.; Silhan, M.; Nachtigall, P. *J. Chem. Phys.* **2002**, *117*, 9298.
- (20) Meyer, F.; Chen, Y. M.; Armentrout, P. B. *J. Am. Chem. Soc.* **1995**, *117*, 4071.
- (21) Davidova, M.; Nachtigallova, D.; Nachtigall, P.; Sauer, J. *J. Phys. Chem. B* **2004**, *108*, 13674.
- (22) Kresse, G.; Gil, A.; Sautet, P. *Phys. Rev. B* **2003**, *68*.
- (23) Cizek, J. *Adv. Chem. Phys.* **1969**, *14*, 35.
- (24) Sierka, M.; Sauer, J. *J. Chem. Phys.* **2000**, *112*, 6983.
- (25) Eichler, U.; Kolmel, C. M.; Sauer, J. *J. Comput. Chem.* **1997**, *18*, 463.
- (26) Palomino, G. T.; Bordiga, S.; Lamberti, C.; Zecchina, A.; Areal, C. O. Vibrational and optical spectroscopic studies on copper-exchanged ferrierite. In *Impact of Zeolites and Other Porous Materials on the New Technologies at the Beginning of the New Millennium, Pts A and B*; Elsevier: Amsterdam, 2002; Vol. 142, p 199.
- (27) Vaughan, P. A. *Acta Crystallogr.* **1966**, *21*, 983.
- (28) It should be pointed out that this numbering scheme differs from that used in Database of Zeolite Structures: <http://www.iza-structure.org/databases/>, where T1 and T4 positions are switched.
- (29) Nachtigall, P.; Davidova, M.; Nachtigallova, D. *J. Phys. Chem. B* **2001**, *105*, 3510.
- (30) Kresse, G.; Hafner, J. *Phys. Rev. B* **1993**, *48*, 13115.
- (31) Kresse, G.; Hafner, J. *Phys. Rev. B* **1994**, *49*, 14251.
- (32) Kresse, G.; Furthmüller, J. *Phys. Rev. B* **1996**, *54*, 11169.
- (33) Kresse, G.; Furthmüller, J. *Comput. Mater. Sci.* **1996**, *6*, 15.
- (34) Blochl, P. E. *Phys. Rev. B* **1994**, *50*, 17953.
- (35) Kresse, G.; Joubert, D. *Phys. Rev. B* **1999**, *59*, 1758.
- (36) Perdew, J. P.; Chevary, J. A.; Vosko, S. H.; Jackson, K. A.; Pedersen, M. R.; Singh, D. J.; Fiolhais, C. *Phys. Rev. B* **1992**, *46*, 6671.
- (37) Perdew, J. P.; Wang, Y. *Phys. Rev. B* **1992**, *45*, 13244.
- (38) Perdew, J. P.; Burke, K.; Ernzerhof, M. *Phys. Rev. Lett.* **1996**, *77*, 3865.
- (39) Perdew, J. P.; Burke, K.; Ernzerhof, M. *Phys. Rev. Lett.* **1997**, *78*, 1396.
- (40) Becke, A. D. *Phys. Rev. A* **1988**, *38*, 3098.
- (41) Lee, C.; Yang, W.; Parr, R. G. *Phys. Rev. B: Condens. Matter* **1988**, *37*, 785.
- (42) Schafer, A.; Horn, H.; Ahlrichs, R. *J. Chem. Phys.* **1992**, *97*, 2571.
- (43) Rodriguez-Santiago, L.; Sierka, M.; Branchadell, V.; Sodupe, M.; Sauer, J. *J. Am. Chem. Soc.* **1998**, *120*, 1545.
- (44) Feyereisen, M.; Fitzgerald, G.; Komornicki, A. *Chem. Phys. Lett.* **1993**, *208*, 359.
- (45) Eichkorn, K.; Weigend, F.; Treutler, O.; Ahlrichs, R. *Theor. Chem. Acc.* **1997**, *97*, 119.
- (46) Eichkorn, K.; Treutler, O.; Ohm, H.; Haser, M.; Ahlrichs, R. *Chem. Phys. Lett.* **1995**, *242*, 652.
- (47) Eichkorn, K.; Treutler, O.; Ohm, H.; Haser, M.; Ahlrichs, R. *Chem. Phys. Lett.* **1995**, *240*, 283.
- (48) Sierka, M.; Sauer, J. *Faraday Discuss.* **1997**, *41*.
- (49) Nachtigallova, D.; Nachtigall, P.; Sierka, M.; Sauer, J. *Phys. Chem. Chem. Phys.* **1999**, *1*, 2019.
- (50) Rappe, A. K.; Casewit, C. J.; Colwell, K. S.; Goddard, W. A.; Skiff, W. M. *J. Am. Chem. Soc.* **1992**, *114*, 10024.
- (51) Treutler, O.; Ahlrichs, R. *J. Chem. Phys.* **1995**, *102*, 346.
- (52) Gale, J. D. *J. Chem. Soc., Faraday Trans.* **1997**, *93*, 629.
- (53) Dunning, T. H. *J. Chem. Phys.* **1989**, *90*, 1007.
- (54) Woon, D. E.; Dunning, T. H. *J. Chem. Phys.* **1993**, *98*, 1358.
- (55) Dolg, M.; Wedig, U.; Stoll, H.; Preuss, H. *J. Chem. Phys.* **1987**, *86*, 866.
- (56) Antes, I.; Dapprich, S.; Frenking, G.; Schwerdtfeger, P. *Inorg. Chem.* **1996**, *35*, 2089.
- (57) Frisch, M. J.; Pople, J. A.; Binkley, J. S. *J. Chem. Phys.* **1984**, *80*, 3265.
- (58) Amos, R. D.; Bernhardsson, A.; Berning, A.; Celani, P.; L. Cooper, D.; Deegan, M. J. O.; Dobbyn, A. J.; Eckert, F.; Hampel, C.; Hetzer, G.; Knowles, P. J.; Korona, T.; Lindh, R.; Lloyd, A. W.; McNicholas, S. J.; Manby, F. R.; Meyer, W.; Mura, M. E.; Nicklaß, A.; Palmieri, P.; Pitzer, R.; Rauhut, G.; Schütz, M.; Schumann, U.; Stoll, H.; Stone, A. J.; Tarroni, R.; Thorsteinsson, T.; Werner, H.-J. *Molpro*.
- (59) Lindh, R.; Ryu, U.; Liu, B. *J. Chem. Phys.* **1991**, *95*, 5889.
- (60) Deegan, M. J. O.; Knowles, P. J. *Chem. Phys. Lett.* **1994**, *227*, 321.
- (61) QM-pot calculations were carried out with 6-T inner part definition and B3LYP functional.
- (62) We note that adsorption energy calculated with PBE functional should not be compared with experimental results since PBE functional is expected to overestimate the Cu–CO interaction. These calculations were carried out in order to compare QM-pot and periodic DFT models.
- (63) Nachtigall, P.; Bludský, O.; Nachtigallova, D.; Cicmanec, P.; Drobná, H.; Bulanek, R. *Stud. Surf. Sci. Catal.* **2005**.
- (64) Kumashiro, P.; Kuroda, Y.; Nagao, M. *J. Phys. Chem. B* **1999**, *103*, 89.
- (65) Bolis, V.; Maggiorini, S.; Meda, L.; D’Acapito, F.; Palomino, G. T.; Bordiga, S.; Lamberti, C. *J. Chem. Phys.* **2000**, *113*, 9248.
- (66) Pople, J. A.; Schlegel, H. B.; Krishnan, R.; Defrees, D. J.; Binkley, J. S.; Frisch, M. J.; Whiteside, R. A.; Hout, R. F.; Hehre, W. J. *Int. J. Quantum Chem. Symposia* **1981**, *15*, 269.